Personalized Glucose-Insulin Model based on Signal Analysis

Authors

1. Simon L. Goede
   MSc
   Systems Research
   Oterlekerweg 4, 1841 GP Stompetoren,
   The Netherlands
   E-Mail : slgoede@kpnmail.nl

2. Bastiaan E. de Galan
   Assistant Professor PhD M.D.
   Department of General Internal Medicine of
   Radboud University Nijmegen Medical Centre,
   Postbus 9101, 6500 HB Nijmegen,
   The Netherlands
   E-Mail : B.deGalan@aig.umcn.nl

3. Melvin Khee Shing Leow
   MBBS, MMed (Int Med), PhD, FACP, FRCP (Edin)
   Dept of Endocrinology, Tan Tock Seng Hospital, Singapore 308433
   Office of Clinical Sciences, Duke-NUS Graduate Medical School, Singapore
   Lee Kong Chian School of Medicine, Nanyang Technological University, Singapore
   E-Mail: melvin_leow@nuhs.edu.sg

Abstract

Glucose plasma measurements for diabetes patients are generally presented as a glucose concentration-time profile with 15-60 min time scale intervals. This limited resolution obscures detailed dynamic events of glucose appearance and metabolism. Measurement intervals of 15 minutes or more could contribute to imperfections in present diabetes treatment. High resolution data from mixed meal tolerance tests (MMTT) for 24 type 1 and type 2 diabetes patients were used in our present modelling. We introduce a model based on the physiological properties of transport, storage and utilization. This logistic approach follows the principles of electrical network analysis and signal processing theory. The method mimics the physiological equivalent of the glucose homeostasis comprising the meal ingestion, absorption via the gastrointestinal tract (GIT) to the endocrine nexus between the liver, pancreatic alpha and beta cells. This model demystifies the metabolic 'black box' by enabling in silico simulations and fitting of individual responses to clinical data. Five-minute intervals MMTT data measured from diabetic subjects result in two independent model parameters that characterize the complete glucose system response at a personalized level. From the individual data measurements, we obtain a model which can be analyzed with a standard electrical network simulator for diagnostics and treatment optimization. The insulin dosing time scale can be accurately adjusted to match the individual requirements of characterized diabetic patients without the physical burden of treatment.

Keywords: Appearance profile, Model identification, Electrical network model, Simulation, Personalized target, Validation

Highlights :

- We model the glucose appearance in diabetic patients based on the properties of electrical networks.
- We fit the integrating actions from oral meal processing and the gastrointestinal tract to the blood compartment on routinely measured glucose data.
- With the individual established two parameter model, a simulation with public available network simulators can be performed.
- This approach enables clinicians to optimize glucose - insulin profiles for patients with diabetes without the burden of physically invasive tests in the clinic.

1. Introduction

In healthy humans, glucose derangements like hyperglycemia and hypoglycemia are normally prevented by homeostatic control mechanisms of the precise antagonism between pancreatic insulin and glucagon secretion. Besides basal insulin secretion for maintenance of euglycemia under fasting conditions, additional prandial insulin response will occur when ambient glucose concentration exceeds a defined threshold level, G_B, about 4.5-5.5 mmol/L. Euglycemic stability of G_B is preserved by a counter-regulatory feedback loop controlled by glucagon of the pancreatic alpha cells against hypoglycemia

Modeling publications of the last four decades are related to insulin-glucose interactions of which the minimal model (Bergman et al.1979) is one of the most prominent examples. Many variants were investigated for in-silico validation by simulation (Palumbo et al 2013). Depending on the main subject of insulin-glucose interaction, such as glucose- and/or insulin appearance, most models are described using ordinary differential equations. In our view, the influence of the gastrointestinal tract (GIT) as input source of the blood compartment is also of major importance to describe the glucose appearance dynamics and related pancreas responses (Cobelli et al. 2014). Sophisticated models have been proposed by Hovorka et al (2004), Kovatchev et al (2009) and Steil (2013) which were further developed for closed loop artificial pancreas applications. Although these models have at least 12 parameters, they primarily concern the effects of insulin, glucose disposal and control of glucose levels within the euglycemic range, but neglect the gastrointestinal absorption process

In our view and that of others (Cobelli et al. 2014), the influence of the gastrointestinal tract as input source of the blood compartment is also of major importance to describe the glucose appearance dynamics and related pancreas responses.
The number of gastrointestinal glucose processing descriptions is limited and none of these were self identifiable and validated with a resolution better than 15 minute intervals. With coarse time intervals it is difficult to achieve an identifiable physiological model. Furthermore, most models were aimed at the presentation of a generalized model based on population averages for a broad kind of applications.

We developed a simple model that incorporates the individual gastrointestinal behavior of glucose appearance dynamics in plasma which has a close conformity to the underlying physiology and not directly concerned with insulin dynamics. This model has only two independent parameters and is fully identifiable based on the available measured data. Furthermore, we demonstrate the different stages of the glucose appearance, distribution and metabolic decay. This results in a clear view on the time delay differences in individuals regarding the glucose appearance an uptake profiles similar to other publications related to a personalized approach. (Rangaiah et al. 2014), (Kissler et al. 2014)

Individual treatment is becoming more and more important the last years. This is also appreciated in the field of the development of personalized drugs (Wang et al. 2007,

2008a and 2008b). In particular the development of design drugs for the treatment of diabetes type 2 is a striking example. (Ma et al, 2012 and Liu et al. 2013)

From recently acquired clinical data of the Radboud University Medical Centre in Nijmegen, The Netherlands, the plasma glucose profiles of 24 diabetic subjects following a mixed meal tolerance test (MMTT) were available for modeling analysis (Engwerda et al. 2013). This dataset, with sample intervals of 5 minutes, mapped out a detailed picture of glucose appearance and metabolism. The postprandial glucose trajectory in blood is dependent on factors such as digestion and glucose fluxes from oral ingestion, gastrointestinal tract processing, time-dependent absorption and kinetics of glucose disposal to return to the homeostatic level. Inspection of the glucose-time graphical plots revealed a very similar response to those of integrating electrical networks comprising resistors and capacitors. This electrical network conformity opens the possibility to use standard electrical network simulators to investigate the properties of the modeled physiology which can be used as an instrument for clinicians for in silico investigation. Here, we show how well the model predicts the glucose profile after MMTT.

2 Methods

2.1 Input and output signals

For the construction of our model we use a holistic approach which borrows methods developed in electrical network and signal theory Schenkman A.L (2005). Here, we can describe observable variations and changes in the glucose concentrations as a function of time by means of glucose “currents”. The time for glucose transport mimics a resistor, while the storage effect is described by a capacitor. The glucose distribution and decay effects are described by glucose generating and utilization current sources while a load resistor represents the insulin-dependent peripheral tissue uptake.

The glucose input signal contributed by the processed meal is approximated by an integrated step function that results in a continuous rising glucose function during the food intake period and attains a peak after the end of the food intake, followed by a gradual decay. The observed glucose kinetic profiles are governed by both insulin-dependent and insulin-independent compartments. We can calculate the appearance time constant by means of the first 5 to 6 data points and/or the last measured points of the glucose appearance data via a user-defined curve fitting procedure. The most dominant effects during the glucose decay phase, originating from brain glucose utilization, hepatic glucose uptake and production are described by means of current sinks and current sources, while the peripheral insulin-dependent uptake is represented by a load resistor.

From the network signal transfer function, initially expressed as Laplace transforms, we calculate the appearance time function by means of inverse transformation to the time domain. From the results of the appearance function, we can derive the steepness of the glucose input function from the GIT and the hepatic, brain and tissue utilization processes.

The most common observable variable as a function of time from an oral meal is the blood glucose level which can be measured with point-of-care technological means. We can consider the human body as a container in which nutrients (e.g. glucose) can be transported, stored and metabolized. The GIT acts as a processing system governing the entry of nutrients in a specific, individually determined, time-dependent fashion to the blood compartment which serves as a generalized transport and storage system. Upon consumption of a mixed meal, the glucose-time profiles can vary depending on the stage and rate of metabolism which in turn are determined by the insulin/glucagon ratio that varies as a function of circulating nutrients including glucose, free fatty acids and amino acids as well as insulin sensitivity.

In the following, the concentrations of substances as a function of time are regarded as signals. The blood circulation, being a 'glucose container', acts as a capacitor with a defined capacitance and receives a time-dependent glucose signal in units of mmol/L/sec. The signal path is depicted in Fig. 1.

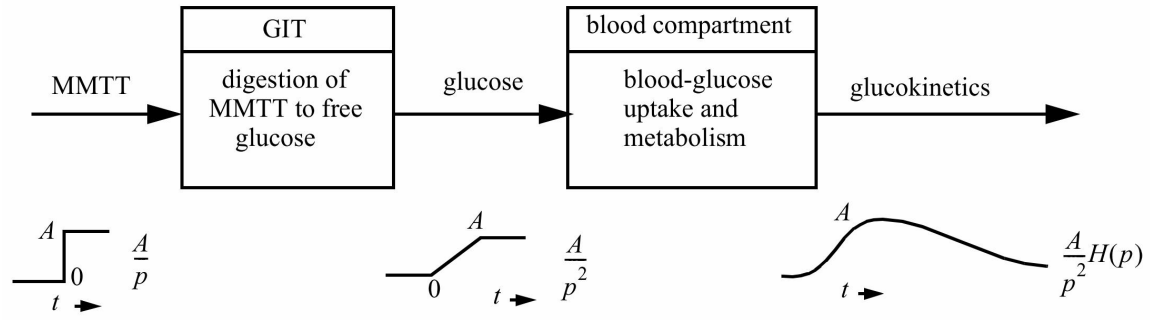

Fig. 1 Glucose signal processing, tracing the path of glucose from the digestion of a mixed meal (MMTT) in the GIT to its trajectory in the circulation according to the principles of glucokinetics. Each time-function pictograms and its associated Laplace transformed signals are illustrated at every stage.

From Fig.1, we appreciate that the mixed meal, considered as a meal bolus, is approximated by a step function $A\varepsilon(t)\ \ 0 < t < t_1$ resulting in a Laplace transformed presentation, A/p, and A represents the maximum amount of the food bolus. The GIT operates as a one directional integrating food to glucose converter from which the glucose signal as a function of time is represented by a ramp function,

$$f_g(t) = \frac{A}{t_1} t\ ,\ 0 < t < t_1 \qquad (1)$$

with the Laplace transformed presentation A/p^2. This signal is the input of the blood compartment capacitor via an input resistance. The input resistance is represented by the physiological effect of time necessary to transport a defined amount of material from one location to another with the dimension sec/L.

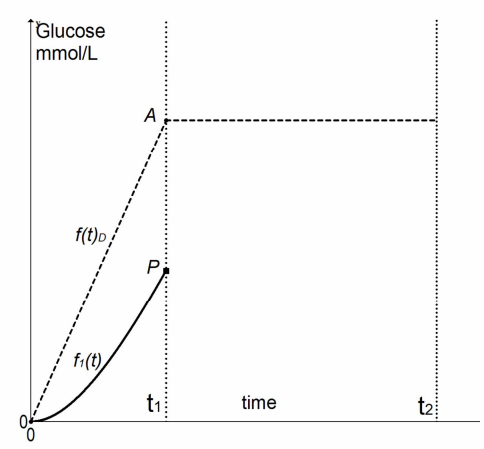

Fig. 2a integrating network response as solid line on a ramp input function (dashed line) The integration action lasts until $t = t_1$ and ends in point P

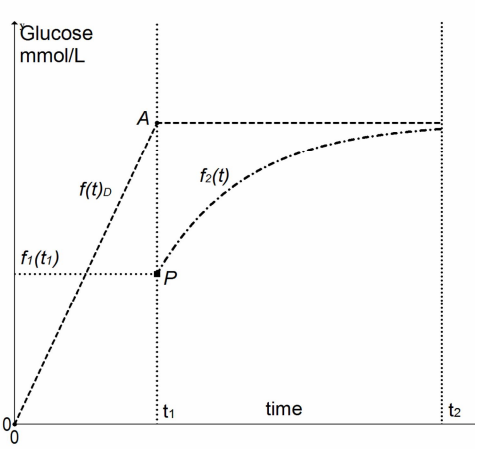

Fig. 2b Dotted dashed line response $f_2(t)$ as translated first derivative of $f_1(t-t_1)$ from point P in $t = t_1$ until $t = t_2$

Fig. 2a presents the integrating network response on a slanted line with maximum value A. The driving function $f(t)_D$ will be the approximated representation of the GIT glucose output.
In Fig. 2b the translated first derivative of $f_1(t-t_1)$ is depicted as the second part of the appearance function and behaves like a response of a first order integrating network on a unity step function. The general glucose appearance profile is depicted in Fig. 3 and shows the maximum glucose level A after t_1 minutes, corresponding to the maximum amount of equivalent glucose in the meal bolus.

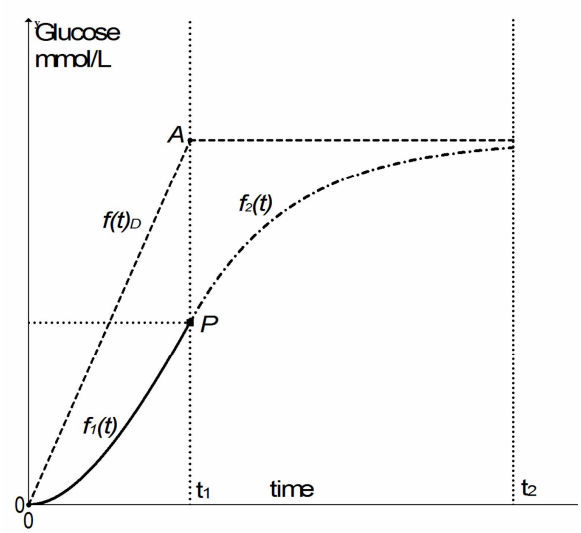

Fig. 3 Linear glucose output $f(t)_D$ from the gastrointestinal process with maximum value A as dashed line with the composed appearance signal $f_1(t)$ as solid line and the related $f_2(t)$ indicated with a dotted-dashed line as a response on this input.

Fig. 3 shows the signal output of the GIT as the dashed line which is approximated as a linearly increasing glucose signal during a defined period t_1 after which the maximum value A is reached and maintained until $t = t_2$. The glucose concentration response, starts at the fasting glucose base level at $t = 0$ with a function $f_1(t)$ (solid line) which is valid until $t = t_1$. At that time the driving function $f(t)_D$, from the GIT, has reached its maximum value A, the rest of the appearance is seamlessly taken over in point P by the saturating translated exponential function $f_2(t)$ (dotted-dashed line) with

$$f_2(t) = f_1(t_1) + \frac{df_1(t-t_1)}{dt} \qquad t_1 < t < t_2 \tag{2}$$

and rises to the maximum level A asymptotically.

From the theoretical background of signal processing, this signal seems to be consistent with the way glucose is transported into the circulation from the intestines via the portal vein during a normal meal.
The glucose release from the GIT behaves accordingly as an integration of the meal bolus in time. From that source, the glucose concentration is gradually increasing in the blood as a function of time until the maximum, A, has been reached implying that the meal bolus has been totally digested and processed to measurable glucose appearance.

We formulate the Laplace transformed GIT output signal as the driving function:

$$L\{f(t)_D\} = \frac{A}{p^2} \tag{3}$$

This result provides information about the properties of the time-dependent glucose appearance when we encounter dominant time lags around 10 to 40 minutes. These prominent glucose appearance time lag effects are observed in mixed meal tolerance tests.

2.2 Glucose appearance and decay model

One of the first modeling descriptions applied in glucose-insulin analysis, based on an electrical network, was investigated and published by Min et al in 1984 and Min, G.B, Woo E.J, (1986). They proposed the model depicted in Fig. 4

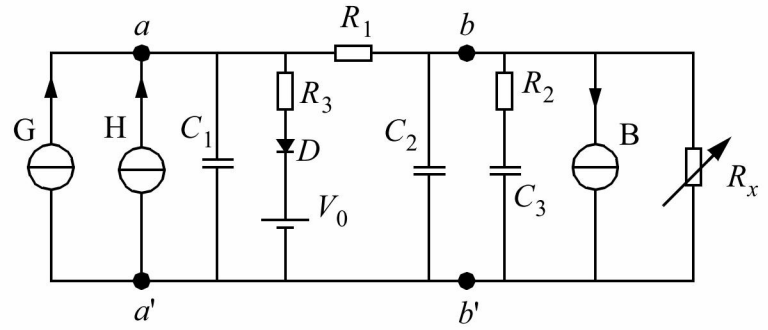

Fig. 4 Electrical schematic representation of glucose - insulin metabolic action according to Min et al. (1984). The compartmental volumes are represented by the capacitances C_1, C_2 and C_3. The rate constants are represented by R_1, R_2, R_3 and Rx. The volume flow rates are represented by the current sources and the currents. The exogenous glucose input current source is represented by G and the hepatic glucose balance by current source H.
The renal secretion is represented by R_3, diode D and excretion threshold V_0.
The value of Rx is directly related to the insulin resistance parameter and varies as a function of the glucose level The current sink B represents the rather constant brain glucose consumption.

The model presentation of Min et al. (1984) and Min, G.B, Woo E.J, (1986) is evaluated for IVGTT glucose responses to establish the values of insulin resistance in four different test groups. They described the glucose currents with current sources where voltages across the resistances are the results of the product of current value and resistor value. This sophisticated model is close to complete, but has the drawback that measured appearance effects in blood glucose levels are difficult to trace back to a specific part of the schematic and thus the related physiology. However, the presented method for simulation is still actual and has great value for individual optimization methods.

In an overview of the current status of research in glucose - insulin models, (Chee F, Fernando T, 2007) most of the glucose appearance profiles provide scarcely detailed or

non existent postprandial glucose appearance profiles where the modeling emphasis was directed to the glucose- insulin metabolism during the glucose decay phase.

With our modeling approach, we generated novel insights previously not reported in existing literature. We investigated the time-dependent appearance of glucose as an indirectly observable signal from the GIT, which can be applied to the blood compartment and can be interpreted as an integrating electrical network function.
All resistances and capacitances are integrated in a single load resistor, a discharge resistor and a capacitor. The network elements are derived from the established system time constant and are directly translatable to physiological processes and functions.
From the analyzed data we interpret the glucose processing by means of a signal description. In this manner, the GIT compartment and the blood compartment have an integrating character.

This glucose appearance and utilization behaviour can be modeled with an alternative electrical circuit, compared to the presentation of Min et al in 1984 and Min, G.B, Woo E.J, (1986) with similar integrating properties (Schenkman A.L 2005).
One major difference compared to the model of Fig. 4 is the addition of the gastrointestinal effect represented by voltage source U in Fig. 5 and the mixed meal test which results in the striking differences between the participants of the Radboud University trial. (Engwerda et al. 2013)
From the data set of a tested person, we calculate the appearance time constant τ by means of a saturating exponential curve fitting procedure with the free available tool Graph 4.4.2 downloadable from the internet (Johansen J, Graph 4.4.2. 2014). The details of the fitting procedure will be discussed in section 2.3.
This time constant applies also to the first part of the appearance curve. With these operations, we also find the ramp coefficient for the driving function. Input and output signals are triply verified in real time by calculation, by scaled hardware simulation using electronics-circuitry and by means of a circuit simulator (SIMetrix Technologies Ltd, 2014) The endocrine dynamics and belonging signal behavior can now be described with an electrical network where the time domain functions are transformed to the $j\omega$ domain or complex frequency p, with the Laplace transform.
After solving the algebraic network equations in the Laplace domain, the analyzed results can be inversely transformed back to the time domain.

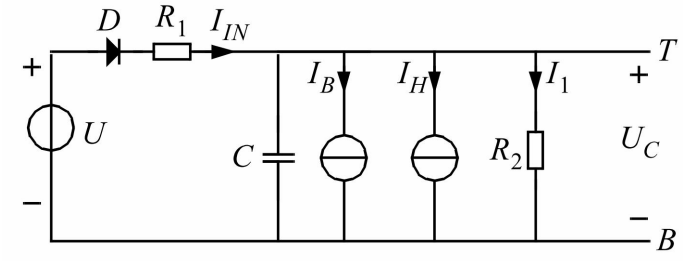

Fig. 5 Elementary electrical circuit equivalent with the capacitor C representing the blood compartment. *U* represents the GIT output signal, diode *D* represents the unidirectional flow of glucose processing. R_1 represents the resistance between GIT

compartment and the blood compartment, which is represented by capacitor *C*. I_B represents the brain glucose current. I_H represents the hepatic balance and I_1 the insulin dependent tissue glucose uptake with R_2 as equivalent for insulin dependent metabolization also known as insulin resistance.

In Fig. 5, the electrical circuit represents the physiological model equivalent of the blood compartment. The glucose concentration as a result of digested carbohydrates from the GIT tract, *G mmol/L*, is equivalent to an electrical voltage source *U*. Diode *D* prevents back flow because the metabolic conversion processes of food to glucose results are essentially irreversible. Resistor R_1 represents the resistance from the GIT compartment to the general blood compartment with the unit sec/L. Capacitor *C* represents the total volume of this blood compartment, which is defined as 80 mL/kg while R_2 stands for resistance to peripheral glucose uptake via insulin-dependent glucose transporters and insulin-independent mechanisms. A high value of R_2 (eg. high insulin resistance) indicates a low discharge current and thus a slow decay of the glucose level. A small value of R_2 (eg. high insulin sensitivity) has the opposite effect. Glucose currents will be translated with the dimension of mmol/sec.

In normal subjects, the rise of the glucose concentration level, equivalent to the rise of the voltage level of *C*, results in a proportional rise of insulin and accordingly the hepatic uptake current source I_H is activated.
In Fig. 5 the indication of the hepatic I_H and brain currents I_B is directed from point *T* to point *B*, resulting in a falling level of U_C.
The hepatic uptake is initiated when a certain, individually determined, threshold level of glucose has been exceeded. When the glucose falls below the hepatic threshold accompanied by a physiological decline in plasma insulin concentration to a level that abrogates its inhibition on hepatic glucose output, the liver will produce glucose. This mechanism will be modeled as a reversal sign of the hepatic current source with a direction from *B* to *T*, which is mainly observable in normal subjects where the glucose decay gradient will be reduced at the moment the liver starts producing glucose.

Brain glucose current I_B will remain relatively constant (Gaohua L, Kimura H, 2009) and is considered independent of the insulin level as glucose uptake into brain tissues is mediated mainly via insulin-independent glucose transporters. Furthermore, I_B is maintained by the hepatic gluconeogenesis in the fasting state resulting in a negative sign for I_H. Resistance is defined as the time it takes to pass a defined amount of material, from one place to another, with the dimension of seconds/Liter and is equivalent to the electrical element *R* in Ohms. The inverse of resistance is defined as conductance with the dimension of Liter/sec.
The glucose current is defined as I_G with the dimension mmol/sec and equivalent to the electrical current measured in ampere.

We use the following equations in analogy from electrodynamics theory.

The amount of glucose

$$g = C.U \text{ mmol} \tag{4}$$

The transported amount of glucose per unit of time

$$I_G = \frac{dg}{dt} \text{ mmol/sec} \tag{5}$$

This results in a relationship between the capacitor current and capacitor voltage

$$I_G = I_C = C\frac{dU_C}{dt} \text{ mmol/sec} \tag{6}$$

The glucose concentration level G is equivalent to a voltage value U mmol/L
The expression of (4) forms the basis of all related differential equations describing the dynamics of the glucose behavior.
To avoid unnecessary complexity in the calculations, the related differential equations will be presented as Laplace transformed expressions.

With

$$\frac{d}{dt}U_C = pU_C \tag{7}$$

the Laplace transform of the capacitor impedance results in

$$Z_C = \frac{U_C}{I_C} = \frac{1}{pC} \tag{8}$$

with p as the complex frequency $p = j\omega$

The resistor is defined as

$$R = \frac{U}{I} \text{ sec/L} \tag{9}$$

We will relate the capacitor value proportionally to the individual body weight according C = 80mL/kg (Min, B.G et al. 1984) representing the volume of the blood compartment. Based on the capacitor value we can derive the values for the belonging resistors R_1 and R_2 and the current sources I_B and I_H. With these relationships, we can translate the physiological parameters to electrical network elements and vice versa. The electrical network elements R_1, R_2 and C have fixed values for an individual and represent mainly the model parameters for the appearance phase. In the time domain, U represents the input signal in the form $f(t)_D = At$ for the time interval $0 < t < t_1$ as shown in Fig. 3.

Based on the Laplace network equations with omission of diode *D* and the current sources I_B and I_H we find:

$$I = I_{R1} = \frac{U}{R_1 + R_2 // Z_C} \tag{10}$$

$$R_2 // Z_C = \frac{R_2 Z_C}{R_2 + Z_C} = \frac{R_2 / pC}{R_2 + 1/pC} = \frac{R_2}{pR_2C + 1} \tag{11}$$

then

$$I = \frac{U}{R_1 + \frac{R_2}{pR_2C + 1}} = \frac{U(pR_2C + 1)}{R_1(pR_2C + 1) + R_2} \tag{12}$$

For the output voltage we find

$$U_C = (R_2 // Z_C)I = \frac{R_2 U}{R_1(pR_2C + 1) + R_2} \tag{13}$$

From which we derive

$$\frac{U_C}{U} = \left(\frac{R_2}{R_1 + R_2}\right)\frac{1}{(p\tau + 1)} \tag{14}$$

Appearance time constant τ is denoted as

$$\tau = \left(\frac{R_1 R_2}{R_1 + R_2}\right)C \tag{15}$$

The decay time constant τ_D without the influence of glucose decay current sources: I_B , I_H and a decoupling of *U* by diode *D* results in

$$\tau_D = R_2 C \tag{16}$$

In a network simulator, the values for resistance and capacitance are related to the seconds-scale, so this implies that after a simulation, a scaling factor of 60 seconds-to-minutes, has to be performed.

Going back to the model depicted in Fig.4, we can derive the appearance characteristic for an MMTT. The glucose release is presented as a linear function of time.
This can be presented according to Fig. 5.

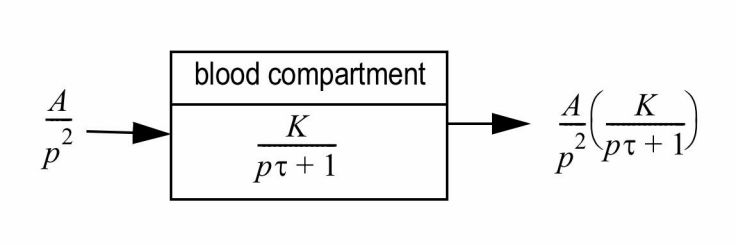

Fig. 6 Laplace-transformed signal transfer with A/p^2 as input signal for the blood compartment resulting in output $(KA/p^2)/(p\tau + 1)$.

At first, we use the following basic Laplace transform for the output of the GIT. For diabetic patients $R_2 >> R_1$, which is valid for most cases, ten we can we approximate

$$K = \frac{R_2}{R_1 + R_2} \approx 1 \tag{17}$$

We find for the Laplace transformed signal *U*:

$$U(p) = \frac{A}{p^2} \tag{18}$$

The output signal $U_C(p)$ represents the measured values of the glucose concentrations in the blood compartment.

$$U_C(p) = \frac{AK}{p^2(p\tau+1)} = \frac{AK}{p^2} - \frac{AK\tau}{p} + \frac{AK(\tau)^2}{p\tau+1} = \frac{AK}{p^2} - \frac{AK\tau}{p} + \frac{AK\tau}{p+1/\tau} \tag{19}$$

, transformed to the time domain:

$$\text{with } a = \frac{1}{\tau}, \tag{20}$$

The S shaped function $U_C(t)$ is composed of two partial functions.
For $K = 1$ we can write the first part with an output range defined by

$$f_1(t) = U_{C1}(t) = A\left[t - \tau\{1 - \exp(-at)\}\right] \text{ for } 0 < t < t_1 \tag{21}$$

as indicated in Fig.2a.
From $t = t_1$ the input function $f(t)_D$ will not rise anymore and remains at the end level *A*.
The second part of the response is described by

$$f_2(t) = U_{C2}(t) = U_{C1}(t_1) + \{A - U_{C1}(t_1)\}\left\{1 - \exp\left(-a(t - t_1)\right)\right\} \qquad t_1 < t < t_2 \tag{22}$$

and represents the saturating part of the appearance response.

In order to connect $U_{C1}(t)$ seamlessly in $t = t_1$ to $U_{C2}(t)$ the following condition has to be met.

$$\frac{d[U_{C1}(t_1)]}{dt} = \frac{d[U_{C2}(t_1)]}{dt} \tag{23}$$

This results in an S-shaped response curve of which the beginning part $0 < t < t_1$ has a different shape compared to the second part with $t_1 < t < t_2$ and is in general asymmetrical. The time signal $U_C(t)$ is determined by three parameters, A, K and τ. Parameter τ, as an internal individual parameter, is furthermore determined by the network model parameters R_1, R_2 and C. From glucose values of a test, the model parameters can be derived with a nonlinear curve fitting procedure based on the parameterized function of (23) from which the obtained value of τ will be applied to the first part of the glucose appearance, $f_1(t)$.

2.3 Fitting procedure

The following procedure results in a correct fit on measured data.
At first the dominant appearance range is determined by the maximum measured glucose values in order to find the system time constant τ, the maximum glucose concentration A and the intersection point with the base line at t = b. For this part we will use the differentiated form of equation (21).
In Fig. 7 we depict the example of patient P01.

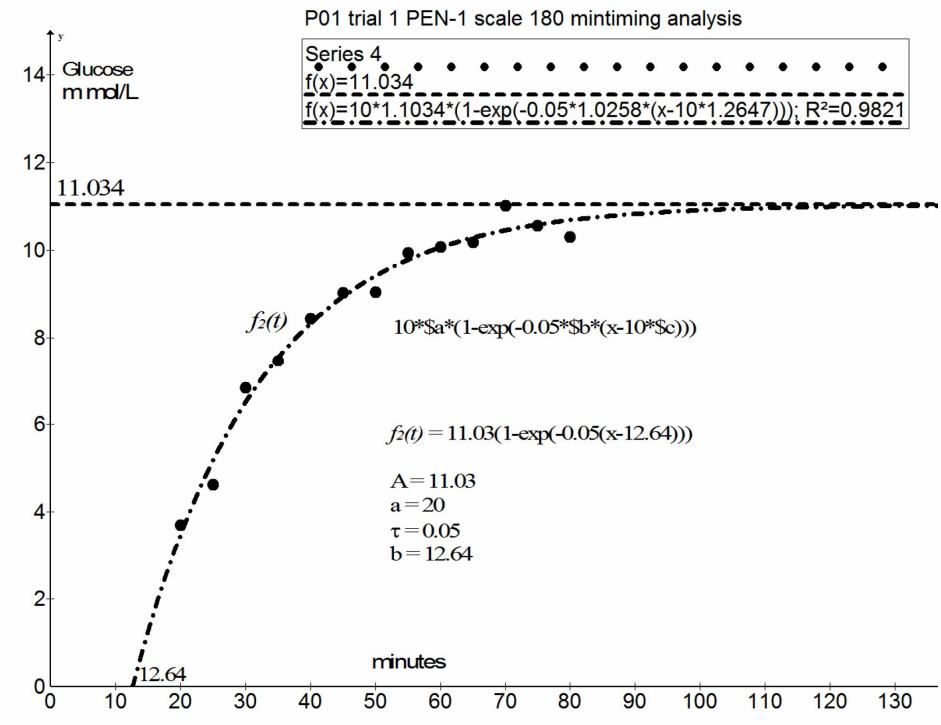

Fig. 7 Fitting procedure starting with the second part $f_2(t)$ of the glucose appearance on the measurements of 20 minutes until 80 minutes, according to the differentiated form of equation (22).
The fitting result for this case, with $R^2 = 0.98$ is depicted as a dashed - dot line intersecting the base level on b = 12.64 minutes. The maximum level A is indicated with the dashed line on 11.034 mmol/L. The extracted time constant $\tau = 20$ minutes with $a = 1/\tau = 0.05$.

The parameterized fitting function for application in Graph 4.4.2 is written as

$$f_2(t) = p*\$a*(1-\exp(-q*\$b*(t-p*\$c))) \tag{24}$$

Where p and q are scaling constants and for this application chosen as p = 10 and q = 0.05 resulting in

$$f_2(t) = 10*\$a*(1-\exp(-0.05*\$b*(t-10*\$c))) \tag{25}$$

The belonging value for the time constant τ is found from $\tau = 1/q*\$b$, the intersection point with the base line is then $b = p*\$c$ and the maximum glucose saturation level $A = p*\$a$

As the second step in the fitting procedure, the first part, $f_1(t)$, of the glucose appearance is then found according to the description depicted in Fig. 8.

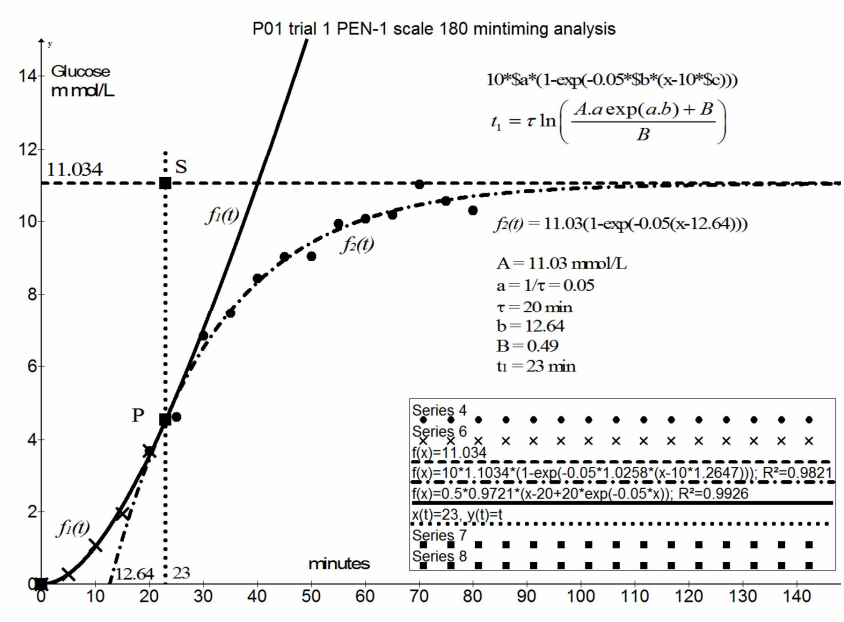

Fig. 8 Fitting procedure according to the form of equation (22) over the first series of measurements from 0 to 20 minutes. The second stage of the fitting procedure is depicted as the solid black line starting in point (0,0) and indicated as $f_1(t)$ with fitting quality R^2 = 0.98 which has one common point P with $f_2(t)$ which can be calculated with the identified parameters A, a, τ, b and B, shown in the figure. With B as multiplication factor of $f_1(t)$. The vertical which starts in t1 = 23 minutes identifies the saturation point S(t_1, A)
The fitting function for $f_1(t)$ is written according to the form of equation (21) where the value for τ from the first fitting operation of $f_2(t)$ is incorporated.

$$f_1(t) = s*\$a*(t-\tau+\tau*\exp(-t/\tau)) \qquad (26)$$

with s = 0.5 as a chosen scaling constant, the fitting function is then

$$f_1(t) = (0.5)*\$a*(t-\tau+\tau*\exp(-t/\tau)) \qquad (27)$$

resulting in

$f_1(t)$ = 0.5*$a*(t-20+20exp(-0.05t)) (28)

after this procedure we find the amplitude of $f_1(t)$ as B = 0.5*$a

For a correct operation in Graph 4.4.2 the variable *t* should be replaced by *x*.
In order to find the value of t_1 we use the equation of (23) which implies that

$$\frac{df_1(t)}{dt} = \frac{df_2(t)}{dt} \quad \text{in } t = t_1 \tag{29}$$

Then we derive

$$t_1 = \tau \ln\left(\frac{a.A.\exp(a.b) + B}{B}\right) \tag{30}$$

which results in the complete set of conditions how the glucose appearance can be constructed from the measured data.
The final result is depicted in Fig. 9.

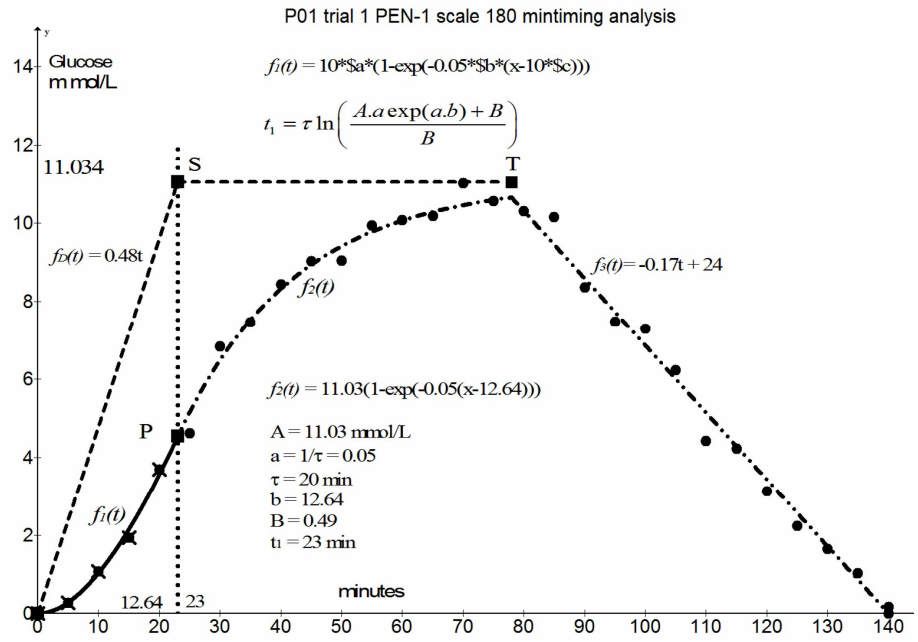

Fig. 9 Complete reconstruction of the fitted data including the driving function $f(t)_D$ = 0.48t as dashed line and the linear decay $f_3(t)$ = -0.17t + 24 as dash dot- dot dash line. The glucose saturation level is maintained at 11 mmol/L from point S to point T (55 min).

Table 1 Glucose test data of P01, time in minutes

P01													
Time minutes	**0**	**5**	**10**	**15**	**20**	**25**	**30**	**35**	**40**	**45**	**50**	**55**	**60**
mmol/L	0.01	0.28	1.07	1.94	3.7	4.62	6.84	7.46	8.43	9.03	9.04	9.94	10.07
Time minutes	**65**	**70**	**75**	**80**	**85**	**90**	**95**	**100**	**105**	**110**	**115**	**120**	**125**
mmol/L	10.18	11.01	10.56	10.3	10.15	8.36	7.48	7.3	6.23	4.43	4.23	3.14	2.25

3 Results

The institutional review board of the Radboud University Medical Centre in Nijmegen, The Netherlands, approved the experimental protocols of MMTT for 24 diabetes patients. (Engwerda et al. 2013) All participants provided written informed consent. The study enrolled type 1 or insulin-treated type 2 diabetes patients tested on two occasions. Before the experimental days all patients were instructed to reduce basal insulin replacement therapy to avoid nocturnal hypoglycemia. Before the tests in the clinic, the patients were in fasting condition at 7.30 a.m. and received intravenous insulin as required to achieve stable euglycemia. After 30 minutes, patients received an individualized dose of subcutaneous insulin and thereafter invited to ingest a meal consisting of 538 kcal, 108 g carbohydrates, 7 g fat and 11 g protein within 15 minutes. During the course of the next three hours, at intervals of five minutes, the individual glucose levels were measured and recorded and for another three hours, the measurements were performed at 10 minute intervals.

3.1 Model simulation based on data of a subject with type 1 diabetes mellitus.

According to the previous modeling results we can verify the measured results and the mathematical formulated model with the Simetrix electrical network simulator.
The value for the extracted time constant τ determines the product of R_1.C. because the value of R_2 is relative large compared to the value of R_1, the influence of R_2 will be negligible. In Fig. 10 we present the simulation schematic used in Simetrix for this simulation.

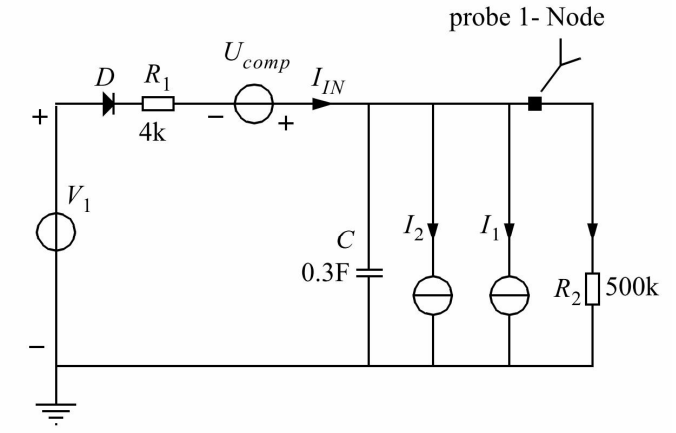

Fig. 10 Representation of the real time simulation network. The driving voltage V_1 starts at t = 0 and rises linearly to 11 volt until t = 1380 sec (23 minutes). This voltage level is maintained until 4680 sec (78 minutes). From that time the constant current source I_1 = 0.8 mA is activated, responsible for the linear decay and shuts down at t = 8400 sec.

The constant brain glucose current I_2 = 20 µA of which the voltage offset effect $R_1.I_2$ is compensated by the voltage source U_{comp} = 0.4 V. The output glucose level is represented by the probe 1 - Node.

The simulated result from the presented network of Fig. 10 is depicted in Fig. 11.

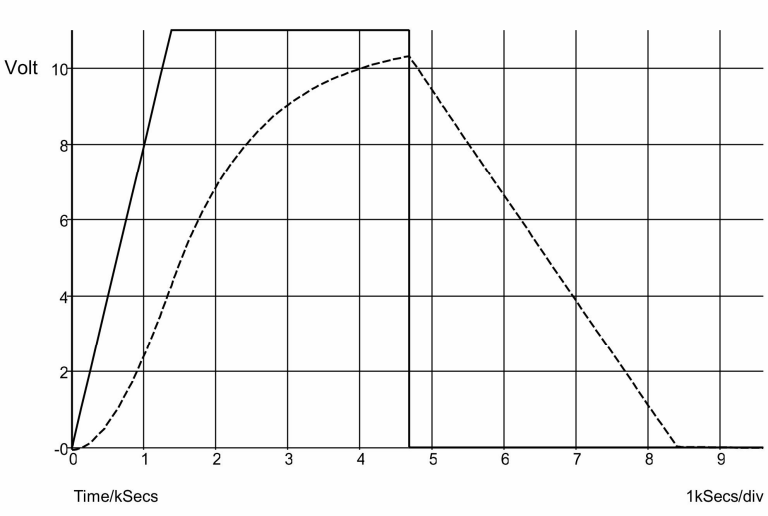

Fig. 11 Simulation result with C = 0.3 F, R_1 = 4k, R_2 = 500k. The driving source V_1 is represented by the solid line, the glucose variations are depicted as a dashed line. The horizontal time axis is presented in a seconds scale, with 1000 sec per division. The vertical axis in volts corresponds with the glucose concentration in mmol/L.

The results from the previous analysis can be translated to physiological parameters. The constant decay is determined as - 10 mmol/3720 sec = $2.68.10^{-3}$ mmol/sec and is equivalent to 0.8 mA. The capacitance value, assuming a bodyweight of 80 kg results in C = 80.80 = 6400 mL or 6.4L. With the established time constant of τ = 20.60 = 1200 sec we calculate the series resistance R_1 = 1200/6.4 = 187 sec/L equivalent to 4kΩ. The correspondence between the glucose concentration is one to one as mmol/L = Volt.

From a physiological perspective, resistor R_2 may not necessarily have the proposed constant high value depicted in Fig 10. However, this model of an average glucose concentration decay with a constant current source is a reasonable approximation as it depicts and represents well all the studied decay patterns as we had illustrated. A closer look at the decay data shows a time and glucose level-dependent modulation of the value of R_2 identical to the approach of Min's R_x model in Fig. 4, which is caused by subcutaneously injected insulin. We observe a resistive mediated negative exponential decay with 4 or 5 interruptions demonstrating the variation in time and glucose level caused by insulin. In other words, the current source action can be interpreted as a resistive discharge where the insulin resistance influences glucose uptake in a manner that results in a virtually constant decay rate without a usual negative exponential profile.

3.2 Overview of obtained model parameters and analysis results

Table 2 provides an overview of the analyzed measured data from most participants. The dataset of participants 4, 5, 8, 12, 18 and 21 were too irregular or incomplete to perform a reliable analysis.
Because the individual body weight was not available in the data set we choose to standardize the capacitor value based on an average body weight of 80 kg resulting in a capacitor of 6.4 L. The variation in time constants τ will then be expressed in the physiological variation of the transport resistor R_1.

Table 2 model and circuit parameters with on C = 6.4L resulting in C = 0.3F

P#	Insulin units	τ min	A mmol/L	t_1 min	t_2 min	t_{end} min	I_3 mmol/sec x 10^{-3}	I_3 µA	R^2	R_1 sec/L	R_1 kΩ
01	11	19.6	11	23	75	140	2.80	800	0.97	187	3k9
02	14	11.28	5.23	24	110	220	0.80	250	0.98	105.7	2k25
03	16	15.76	10	14.8	135	230	1.75	507	0.99	147.7	3k15
06	9	22.22	10	15	125	360	0.70	203	0.97	208.3	1k8
07	24	40	10.45	26.8	155	390	0.74	214	0.97	375	8
09	18	22.9	5.55	22.2	110	210	0.93	270	0.99	214.7	4k58
10	12	11.63	7.25	10.5	51	120	1.75	507	0.98	109	2k34
11	8	11.76	9	17.5	62	160	1.53	445	0.98	110.3	2k35
13	40	20	8.8	20	70	155	1.73	501	0.96	187.5	4
14	18	14.3	7.7	16.3	80	175	1.35	391	0.99	134	2k86
15	17	11	9.5	15	60	190	1.22	353	0.98	103	2k2
16	24	11	6.25	8.3	40	80	2.60	754	0.97	103	2k2
17	8	33.3	13.8	24	80	280	1.15	333	0.99	312	6k66
19	14	50	11.55	23	145	340	0.99	287	0.97	468.8	10
20	13	33.3	8.55	13.8	150	285	1.05	304	0.97	312	6k66
22	20	7.14	5	14.4	45	160	0.72	208	0.98	66.9	1k43
23	18	33.3	14.9	14.5	100	260	1.55	450	0.99	312	6k66
24	12	6.67	2.9	15	27	90	0.77	223	0.97	62.5	1k33

4 Discussion

The detailed glucose appearance analysis, resembling the signal behaviour of integrating electrical networks, was possible by the high resolution glucose appearance and decay measurements with intervals of 5 minutes for diabetic subjects. In comparison with other published models, we applied a mainly graphical presentation and related time function interpretation of glucose appearance data and metabolic effects, demonstrating the identifiable properties of the appearance model by calculating the belonging system time constant τ, the end time of GIT glucose generation t_1 and the maximum glucose concentration. Despite the detailed dataset of the trial which provided the possibility for a solid modeling and high quality of fit for most participants, there were six datasets that could not be analyzed properly because of incompleteness and/or erroneous data.

One of our objectives was to investigate and understand the underlying physiological mechanisms of the GIT glucose processing and the appearance profile made visible by common glucose measurement procedures. From the analysis results presented in Table 2 we encountered a wide variety of glucose appearance profiles and time constants.
For the diabetes patients with the MMTT, the GIT has a pronounced influence on the shape of the glucose appearance. The output of the GIT is the input for the glucose-insulin system in the main blood compartment. The human body is modeled as a so-called "black box" of which the internal metabolic results can be interpreted as a set of logistic events modeled by an electrical network of resistors, a capacitor, a voltage source and current sources. The output response of the electrical network, the capacitor voltage, represents the blood glucose measurements as a function of time. From the MMTT data set, we can calculate the model parameters with a nonlinear curve fitting procedure which demonstrates directly the self identifiability of the model. With these parameters, we reconstruct the complete network equivalent, steepness of the input signal and the belonging limiting values that describe the glucose appearance phase.
Besides the calculation procedure to derive the model parameters and response from measured data, an electrical network simulator showed exactly the same curves as were calculated from the dataset. We also built a real electrical network consisting of a resistor and a capacitor, which demonstrated in a laboratory test bench the same electrical response. We can translate the network elements and their values to relevant physiological parameters.
In all investigated cases we found a more or less constant linear decay of the glucose concentration. This effect is of course due to the administered insulin at the start of the meal test and will become effective after one or two hours. With the available data of starting insulin units we can correlate this amount with the decay effect in terms of a constant discharge current. From the data overview in Table 2 it is clear that the insulin dose and belonging effect is strictly individual.

With the application of an electrical network model of the glucose-insulin system based on the underlying physiology, we can derive the network elements with a curve-fitting algorithm applied to individual glucose data resulting in R^2 values better than 0.95. The model results can be verified with an electrical simulator like SIMetrix. The simulator also provides the possibility to fine tune the parameters in such a way that the simulation result fits the glucose measurements to a satisfying degree, after which the characteristics of the input signal can be found.

The proposed model has only two independent parameters and the model is fully self identifiable based on the measured data. This feature provides a distinct difference compared with earlier published models as Bergman et al.(1979), Palumbo et al (2013), Cobelli et al. (2014), Kovachev et al (2009), Hovorka et al (2004) and Steil (2013) none of which has the property of model identification by individual measured data with only two independent model parameters.

With the proposed and validated model, we showed that the unique individualized appearance behavior is determined by model parameter τ and maximum bolus value A. During the first phase of the curve-fitting, we have the primary time constant of the glucose system which can immediately be applied as a reliable predictor for the rest of the glucose appearance process. Furthermore, we can interpret and translate the results to physiological characteristics that may assist in diagnosis and treatment. The clinician can use this individual characterized model with the aid of a normal standard electrical network simulator without knowledge of the underlying mathematics and operations. The investigation of the data sets of diabetic persons showed a wide variety in glucose profiles and metabolic behavior which indicates that average values for the characterization of a glucose - insulin system will not be usable for individual treatment optimization. Such data supports the application of individualized parameters for clinical management of patients, an approach promulgated by precision medicine initiatives. Our network model characterizes the tested individual with standard glucose measurement methods and provides a characteristic that can be interpreted as a filtered result from measurements and in that sense can predict the glucose profile based on the established time constant. This leads to the conclusion that every person has a specific individual glucose appearance and decay characteristic that can be mimicked and analyzed by the presented model and simulator. This opens the possibility for an optimized individualized treatment for diabetic patients such as the design of better insulin profiles. Furthermore the calculated characteristic model parameters could be used in artificial pancreas implementations. With the data from Table 1 and Table 2, other researchers can verify the quality and validity of the discussed models.

Limitations in our research were the lack of individual body weight data, which has impact on the choice of the capacitor value and thus the feeding resistor value of R_1. Also, the incomplete dataset of participants 4, 5, 8, 12, 18 and 21 impacted the final result. In this study, it would be very instructive to have also similar test data from healthy participants in an MMTT for comparison. We have our focus on the glucose appearance modeling, but the decay mechanisms were not deeply investigated and modeled with a satisfactory constant decay rate using a constant current source. This

model does not directly represent the underlying physiological actions of insulin resistance and molecular kinetics of glucose transporters. Although the insulin resistance is high in diabetic subjects, this value can be surmounted by insulin at higher levels and is a subject for future modeling attempts.
Another limitation is found in the lack of a web based supported simulation environment of which we found examples in related areas of bioinformatics, protein design and medical drug design. Wang et al. (2007), Wang et al. (2008), Wang J.F, Wei D.Q, Li L, (2008), Qiu et al. (2016). Also external modeling expertise has then to be incorporated in the clinical organization.

5 Concluding Remarks

Simulation is increasingly applied as a verification method in many fields of scientific research. The fundamental starting point and reason for existence is found in the real time and real materials costs and efforts reduction aspects without physical invasive events. With a simulation the researcher and clinician can try out several approaches for design and/or treatment without the downfalls of an experimental failure or unnecessary patient burden. We find inspiring examples in the use of web server supported simulation environments like iATC-mISF in bioinformatics, drug and Anatomical Therapeutic Chemical) class/classes research. (Qiu et al. 2016, Chen et al.2016, Cheng et al. 2016, Jia et al. 2016, Qui et al. 2016, Zang et al. 2016)
Important research was also published about simulated properties of phosphorylation in proteins. (Qui et al. 2016, Jia et al.2016).
From these examples we also realize the impact and importance of an easily accessible web server to support the simulation environment necessary for realistic simulations such as in medicinal chemistry. (Chou, 2015)
For such a web-based simulation portal the characterization of individual measurements in a usable simulation model is a fundamental condition.
The development of a web-based simulation environment for the clinical treatment of diabetes patients and a comparison with healthy subjects with similar time intervals is an endeavor for future research.

References

Bergman R.N, Ider YZ, Bowden C.R, Cobelli C (1979) Quantitative estimation of insulin sensitivity. Am J Physiol 236:E667–E677.

Chee F, Fernando T, (2007) Lecture Notes in Control and Information Sciences, Close-Loop Control of Blood Glucose, Springer Verlag
ISBN: 978-3-540-74030-8 (Print) 978-3-540-74031-5

Chen W, Ding H, Feng P (2016) iACP: a sequence-based tool for identifying anticancer peptides. Oncotarget, 2016, 7, 16895-16909.

Cheng X, Zhao S.G, Xiao X, (2016) iATC-mISF: a multi-label classifier for predicting the classes of anatomical therapeutic chemicals. Bioinformatics, 2016, doi: 10.1093/bioinformatics/btw644.

Chou K.C, (2015) Impacts of bioinformatics to medicinal chemistry. Medicinal Chemistry, 2015, 11, 218-234.

Cobelli C, Dalla Man C, Toffolo G, Basu R, Vella A, Rizza R, (2014), The Oral Minimal Model Method, Diabetes. Apr;63(4):1203-13.
doi: 10.2337/db13-1198

Engwerda E.C.E, Tack C.J, De Galan B.E. (2013) Needle-Free Jet Injection of Rapid-Acting Insulin Improves Early Postprandial Glucose Control in Patients With Diabetes Diabetes Care 36: 3436-3441

Gaohua L, Kimura H, (2009) A mathematical model of brain glucose homeostasis, Theoretical Biology and Medical Modelling, 6:26
DOI: 10.1186/1742-4682-6-26

Hovorka R, Canonico V, Chassin L.J, Haueter U, Massi-Benedetti M, Federici M O , Pieber T.R, Schaller H.C, Schaupp L, Vering T and Wilinska M E, (2004) Nonlinear model predictive control of glucose concentration in subjects with type 1 diabetes, Physiol. Meas. 25 (2004) 905–920

Jia J, Liu Z, Xiao X, (2016) iCar-PseCp: identify carbonylation sites in proteins by Monto Carlo sampling and incorporating sequence coupled effects into general PseAAC. Oncotarget, 2016, 7, 34558-34570.

Jia J, Zhang L, Liu Z, (2016) pSumo-CD: Predicting sumoylation sites in proteins with covariance discriminant algorithm by incorporating sequence-coupled effects into general PseAAC. Bioinformatics, 2016, 32, 3133-3141.

Johansen J, Graph 4.4.2 (2014) A graphical mathematical tool.
Last updated: Available as a free download from http://www.padowan.dk/graph/

Kissler S.M, Cichowitz C, Sankaranarayanan S, Bortz D.M, Journal of Theoretical Biology, Volume 359, 21 October 2014, Pages 101-111.

Kovatchev B.P., Breton M, Ph.D., Dalla Man Cand Cobelli C, (2009) In Silico Preclinical Trials: A Proof of Concept in Closed-Loop Control of Type 1 Diabetes Journal of Diabetes Science and Technology Volume 3, Issue 1, January 2009

Liu L, Ma Y, Wang R.L, (2013) Find novel dual-agonist drugs for treating type 2 diabetes by means of cheminformatics. Drug Design, Development and Therapy, 2013, 7, 279-287.

Ma Y, Wang S.Q, Xu W.R, (2012) Design novel dual agonists for treating type-2 diabetes by targeting peroxisome proliferator-activated receptors with core hopping approach. PLoS ONE, 2012, 7, e38546.

Min, B.G, Woo E.J. Lee, H.K, Min, K.H, (1984) Separation of Physiological Factors Influencing Kinetics in Diabetic Patients Using Computer Simulation Method, (1984) Journal of Korean Medical Association, Vol 27, No. 1 1984.

Min, G.B, Woo E.J, (1986) An Electrical Equivalent Circuit Model of Glucose-Insulin Kinetics during Intravenous Glucose Tolerance Test in Dogs and Man.Mathematical Modelling Elsevier Vol. 7 Issues 9 - 12 1986 pages 1187 - 1193

Palumbo P, Ditlevsen S, Bertuzzi A, De Gaetano A, (2013) Mathematical modeling of the glucose-insulin system: A review, Mathematical Biosciences 244 (69 - 81)

Qiu W.R, Sun B.Q, Xiao X, (2016) iPhos-PseEvo: Identifying human phosphorylated proteins by incorporating evolutionary information into general PseAAC via grey system theory. Molecular Informatics, 2016, doi:10.1002/minf.201600010.

Qiu W.R, Sun B.Q, Xiao X, (2016) iHyd-PseCp: Identify hydroxyproline and hydroxylysine in proteins by incorporating sequence-coupled effects into general PseAAC. Oncotarget, 2016, 7, 44310-44321.

Qiu W.R, Xiao X, Xu Z.H, (2016) iPhos-PseEn: identifying phosphorylation sites in proteins by fusing different pseudo components into an ensemble classifier. Oncotarget, 2016, 7, 51270-51283.

Rangaiah G.P, Samavedham L, Balakrishnan N.P, Personalized mechanistic models for exercise, meal, and insulin interventions in children and adolescents with type 1 diabetes, (2014) Journal of Theoretical Biology, 21 September 2014, Pages 62-73.

Schenkman A.L (2005) Transient analysis of Electrical Power Circuits Handbook. Springer USA ISBN 978-0-387-28799-7 DOI 10.1007/0-387-28799-X https://download.e-bookshelf.de/download/0000/0008/76/L-G

SIMetrix Technologies Ltd, (2014) Circuit Simulation, 78 Chapel Street, Thatcham, Berkshire, RG18 4QN United Kingdom, http:/www.simetrix.co.uk

Steil G.M, (2013) Algorithms for a Closed-Loop Artificial Pancreas: The Case for Proportional-Integral-Derivative Control Journal of Diabetes Science and Technology Volume 7, Issue 6, November 2013

Wang J.F, Wei D.Q, Li L, (2007) 3D structure modeling of cytochrome P450 2C19 and its implication for personalized drug design. Biochem Biophys Res Commun (BBRC) (Corrigendum: ibid, 2007, Vol.357, 330), 2007, 355, 513-519.

Wang J.F, Wei D.Q, Chen C, (2008) Molecular modeling of two CYP2C19 SNPs and its implications for personalized drug design. Protein & Peptide Letters, 2008, 15, 27-32.

Wang J.F, Wei D.Q, Li L, (2008) Review: Pharmacogenomics and personalized use of drugs. Current Topics of Medicinal Chemistry, 2008, 8, 1573-1579.

Zhang C.J, Tang H, Li W.C, (2016) iOri-Human: identify human origin of replication by incorporating dinucleotide physicochemical properties into pseudo nucleotide composition. Oncotarget, 2016, 7, 69783-69793.